Supporting Information

Beneficial use of a coordination complex as the junction catalyst in a bipolar membrane

Zijuan Ge,[a] Muhammad Aamir Shehzad,[a] Liang Ge,[a] Yuan Zhu,[a] Huijuan Wang,[b] Geng Li,[a] Jianjun Zhang,[a] Xiaolin Ge,[a] Liang Wu,[,a] and Tongwen Xu*[,a]*

[a] School of Chemistry and Materials Science, University of Science and Technology of China, Hefei, Anhui 230026, China

[b] Experimental Center of Engineering and Material Science, University of Science and Technology of China, Hefei, Anhui 230026, China

*Corresponding author: *Liang Wu*: liangwu8@ustc.edu.cn; *Tongwen Xu*: twxu@ustc.edu.cn.

1. Hydrolysis of PAN

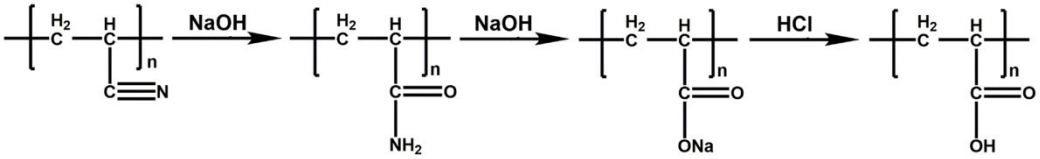

Scheme S1. The hydrolysis reaction indicating the conversion of -CN groups on the PAN membrane surface into -$CONH_2$ followed by into -COONa groups while immersing in alkaline solution. Ultimately, the immersion of the hydrolyzed membrane into an acidic solution leads the conversion of -COONa into -COOH groups.

2. ATR-FTIR spectra

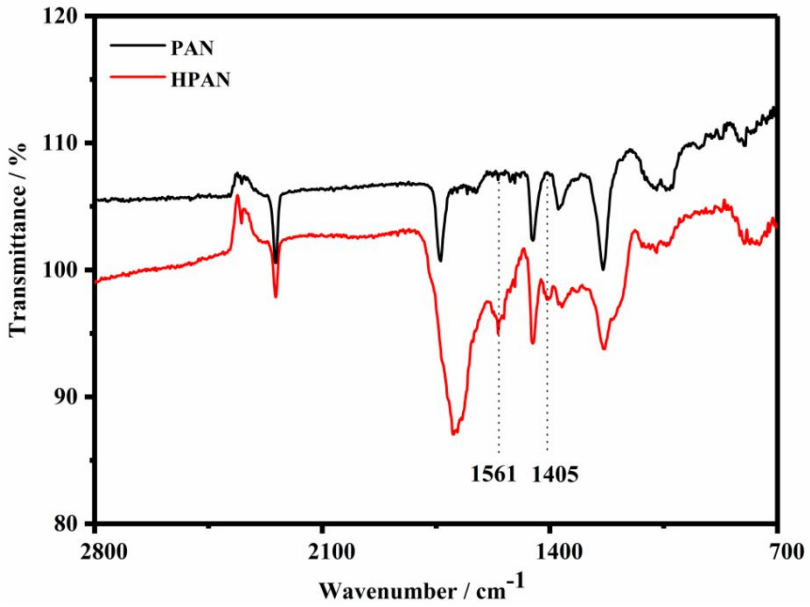

Figure. S1. ATR-FTIR spectra of the PAN and HPAN membranes. The two spectra both show strong peaks at around 2243 cm^{-1} and 1451 cm^{-1} wavenumbers, which are due to the -CN groups. The appeared bands at 1561 cm^{-1} and 1405 cm^{-1} in the spectrum of HPAN membrane provide strong evidence of carboxyl groups after hydrolysis reaction.

3. ^{1}H NMR spectra

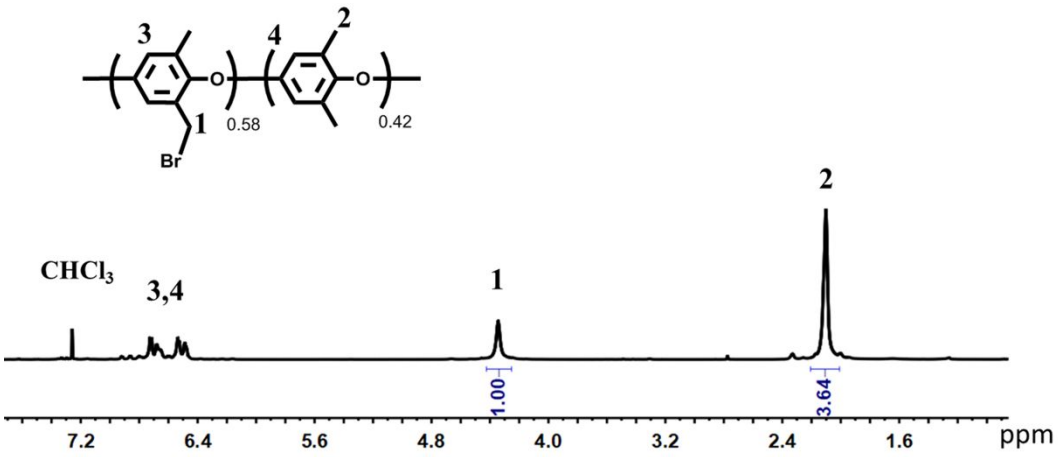

Figure. S2. ^{1}H NMR spectra of BPPO employing $CDCl_3$ as the deuterated solvent.

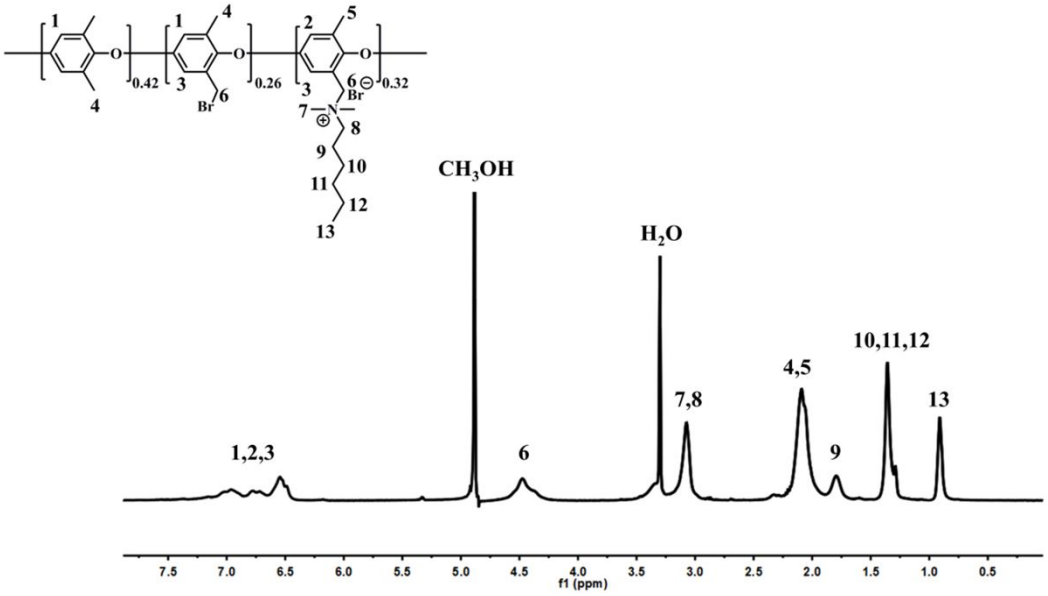

Figure. S3. ^{1}H NMR spectra of QPPO-C_6 using CD_3OD-d_4 as the deuterated solvent.

4. Table S1. Elemental analysis of QPPO-C_6 polymer

Name	Weight (mg)	N (%)	C (%)	H (%)	N Area	C Area	H Area
QPPO-C_6	2.013	2.17	59.16	7.00	1474	27632	11260

$$\frac{m * x * 14}{329 * x + 200 * (0.58 - x) + 120 * 0.42} = m * [N]$$

where x is the actual degree of quaternization reaction, m is the weight of QPPO-C_6 polymer.

5. The digital image of $FeCl_3$ and Fe(III)@PEI complexes solutions.

Figure S4. Digital images of the solutions of Fe(III)@PEI coordination complexes and $FeCl_3$ with the same concentration of Fe(III) ions. Left digital image is of $FeCl_3$ (faint yellow) and the right image is of Fe(III)@PEI complexes (wine-coloured).

6. Current-voltage (I-V) curves measurement

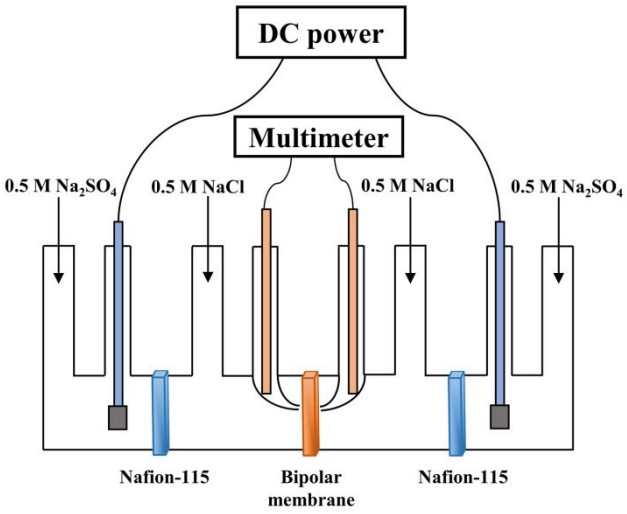

Scheme S2. The experimental setup used for the I-V measurement. The I-V measurement cell includes two pieces of Nafion® 115 and a piece of the prepared bipolar membrane. The active area of this cell is 10.18 cm^2. Two platinum electrodes are employed to supply stable direct current to the whole cell whereas a set of Ag/AgCl reference electrodes is used for recording the transmembrane voltage drop. Na_2SO_4 (0.5

mol L^{-1}) and NaCl (0.5 mol L^{-1}) solutions are used in the electrode compartment and acid/base compartments, respectively.

7. **The EDS spectra of HPAN membrane and Fe(III)@PEI-based HPAN membrane.**

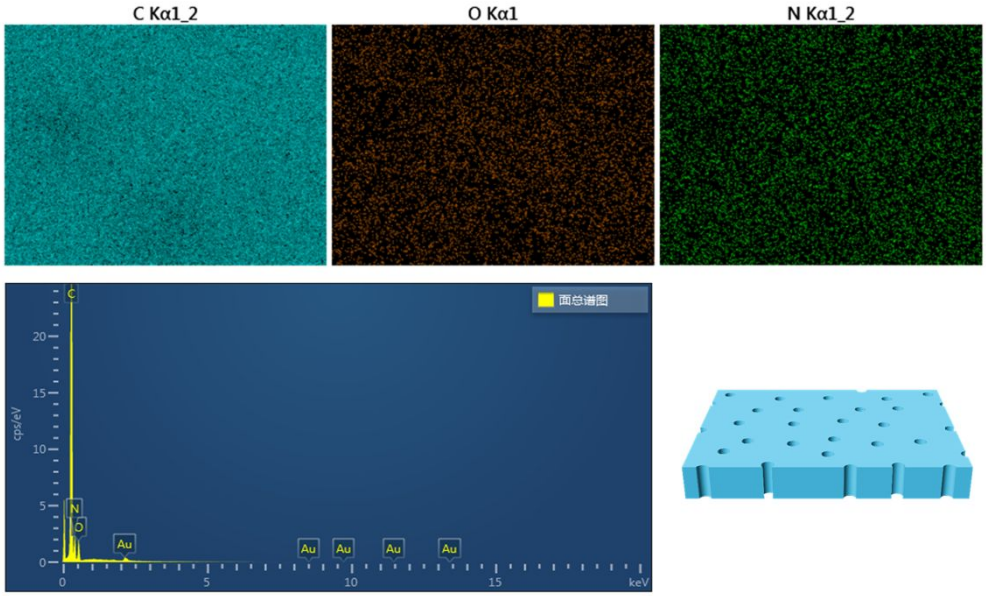

Figure S5. The elemental map and EDS spectrum of HPAN membrane surface. A schematic illustration at the lower right corner is showing the HPAN membrane. The observed three elements (C, N, and O) are derived from the -CN and -COOH groups on the surface of HPAN membrane. The visible minor Au content in the EDS spectrum is due to its spraying on the membrane surface to increase the conductivity of the membrane to avoid a drift SEM analysis.

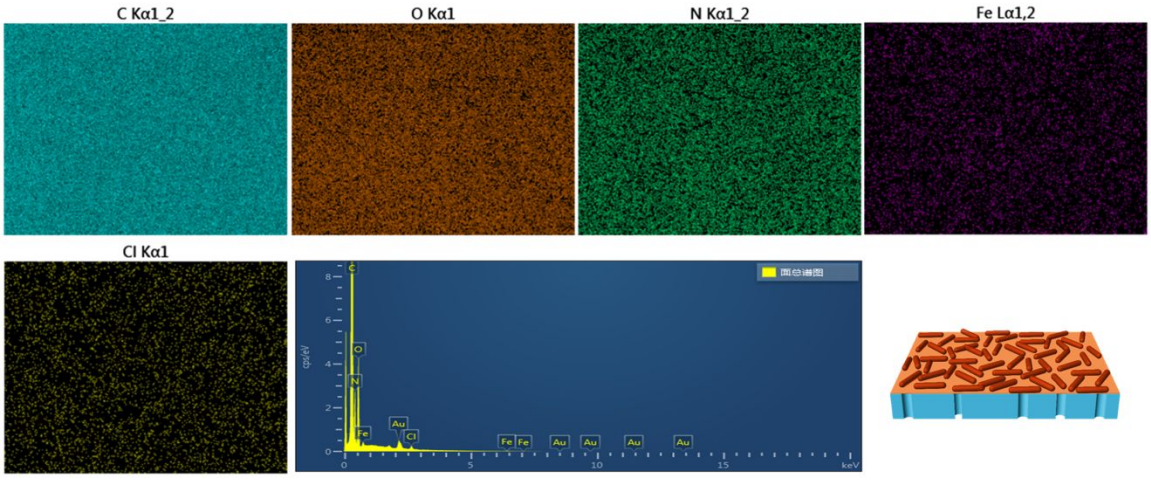

Figure. S6. The elemental map and EDS spectrum of Fe(III)@PEI-based HPAN

membrane surface. A schematic illustration at the lower right corner is showing the Fe(III)@PEI-based HPAN membrane. The found Oxygen (O) element is derived from the -COOH groups on the HPAN membrane. The C and N elements are due to the -CN and -COOH groups on the Fe(III)@PEI-based HPAN membrane and PEI in the Fe(III)@PEI catalyst. The existence of Fe and Cl elements is due to $FeCl_3$ in the Fe(III)@PEI catalyst. The visible minor Au content in the EDS spectrum is due to its spraying on the membrane surface to increase the conductivity of the membrane to avoid a drift SEM analysis.

8. The SEM images, elemental map, and EDS spectra of the bottom surface of the initial HPAN and the Fe(III)@PEI-based HPAN membranes

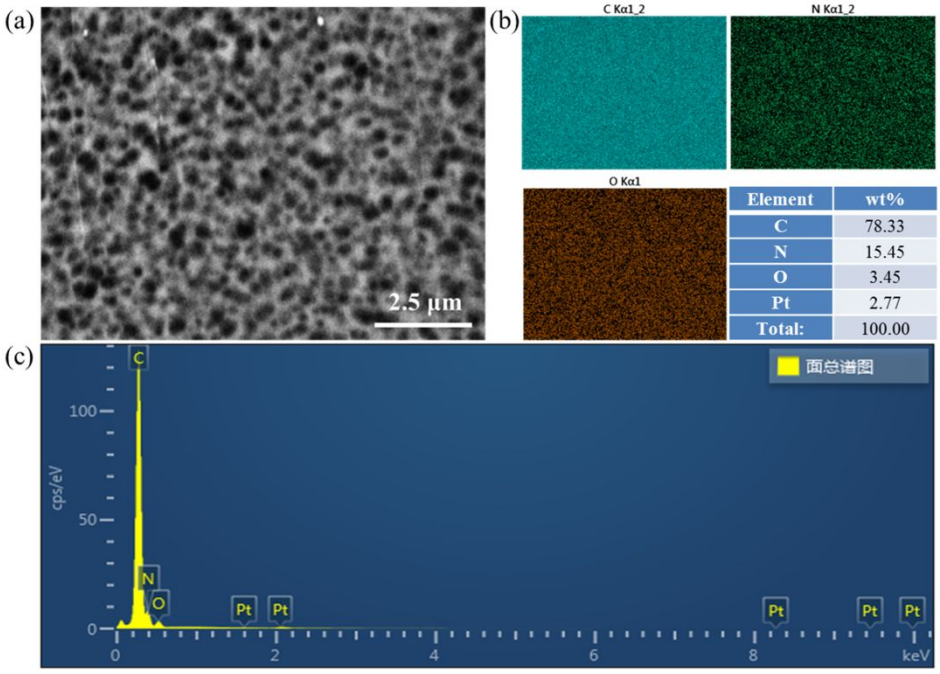

Figure S7. (a) The SEM image of the bottom surface of HPAN membrane. (b) The elemental map of the bottom surface of HPAN membrane. (c) The EDS spectrum of the bottom surface of HPAN membrane. The observed three elements (C, N, and O) are derived from the -CN and -COOH groups on the surface of HPAN membrane. The visible minor Pt content in the EDS spectrum is due to its spraying on the membrane surface to increase the conductivity of the membrane to avoid a drift SEM analysis.

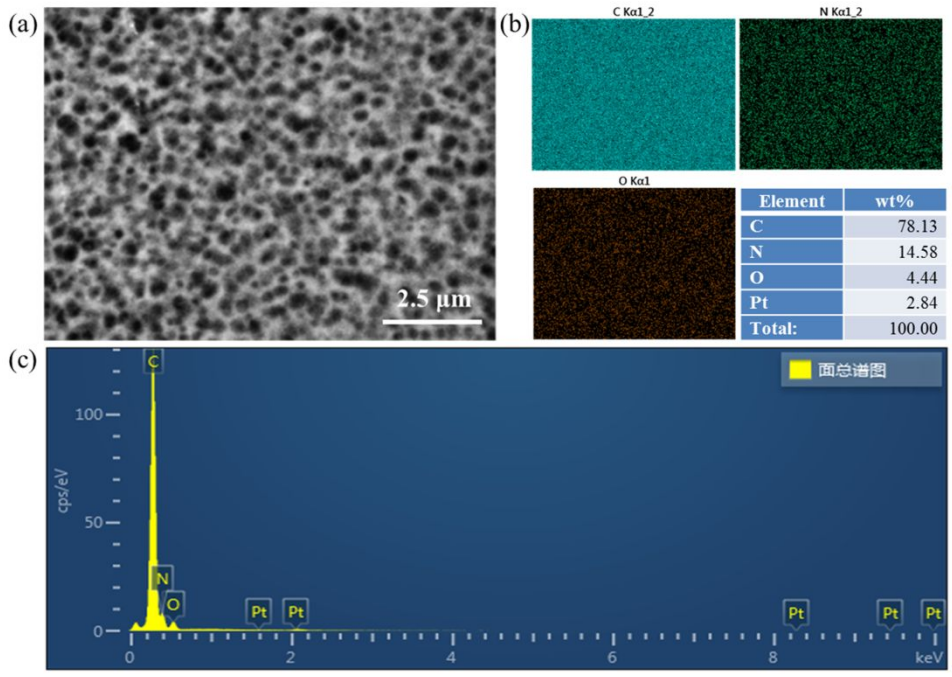

Figure S8. (a) The SEM image of the bottom surface of Fe(III)@PEI-based HPAN membrane. (b) The elemental map of the bottom surface of Fe(III)@PEI-based HPAN membrane. (c) The EDS spectrum of the bottom surface of Fe(III)@PEI-based HPAN membrane. The observed three elements (C, N, and O) are derived from the -CN and -COOH groups on the surface of Fe(III)@PEI-based HPAN membrane. The visible minor Pt content in the EDS spectrum is due to its spraying on the membrane surface to increase the conductivity of the membrane to avoid a drift SEM analysis.

9. **Table S2.** The junction resistance (R_b) of different bipolar membranes.

Membranes	R_∞ (Ω)	R_0 (Ω)	R_b (Ω)
PEI-based BPM	2.19	16.26	14.07
$FeCl_3$-based BPM	0.59	3.11	2.52
Fe(III)@PEI-based BPM	0.63	2.06	1.43

10. Table S3. The depletion region thickness (λ) of different bipolar membranes.

Membranes	Peak (Ln ν,	Peak (ν,	λ (nm)

	-Im(Z))	-Im(Z))	
PEI-based BPM	(6.68, 3.03)	(796.32, 3.03)	54.20
$FeCl_3$-based BPM	(8.29, 0.45)	(3983.83, 0.45)	40.27
Fe(III)@PEI-based BPM	(8.06, 0.39)	(3165.29, 0.39)	27.73